Provided for non-commercial research and education use.
Not for reproduction, distribution or commercial use.

This article appeared in a journal published by Elsevier. The attached copy is furnished to the author for internal non-commercial research and education use, including for instruction at the authors institution and sharing with colleagues.

Other uses, including reproduction and distribution, or selling or licensing copies, or posting to personal, institutional or third party websites are prohibited.

In most cases authors are permitted to post their version of the article (e.g. in Word or Tex form) to their personal website or institutional repository. Authors requiring further information regarding Elsevier's archiving and manuscript policies are encouraged to visit:

http://www.elsevier.com/copyright

Author's personal copy

Applied Surface Science 255 (2008) 3375–3380

Contents lists available at ScienceDirect

Applied Surface Science

journal homepage: www.elsevier.com/locate/apsusc

# Study of the effect of plasma power on ZnO thin films growth using electron cyclotron resonance plasma-assisted molecular-beam epitaxy

Z. Yang, J.-H. Lim, S. Chu, Z. Zuo, J.L. Liu *

*Quantum Structures Laboratory, Department of Electrical Engineering, University of California at Riverside, Riverside, CA 92521, USA*

ARTICLE INFO

*Article history:*
Received 28 April 2008
Received in revised form 3 July 2008
Accepted 22 September 2008
Available online 8 October 2008

*PACS:*
81.05.Dz
81.15.Hi
61.14.Hg
68.37.Yz
78.55.Et

*Keywords:*
ZnO
Molecular-beam epitaxy
Plasma power
ECR
II–VI semiconductors
Growth rate
X-ray diffraction
Photoluminescence

ABSTRACT

ZnO thin films were grown on *r*-plane sapphire substrates using electron cyclotron resonance (ECR) plasma-assisted molecular-beam epitaxy. The effect of the oxygen ECR plasma power on the growth rate, structural, electrical, and optical properties of the ZnO thin films were studied. It was found that larger ECR power leads to higher growth rate, better crystallinity, lower electron carrier concentration, larger resistivity, and smaller density of non-radiative luminescence centers in the ZnO thin films.

© 2008 Elsevier B.V. All rights reserved.

## 1. Introduction

Recently, ZnO has been widely studied for its attractive applications in ultraviolet light-emitting diodes and laser diodes, because it has a direct bandgap of 3.37 eV at room temperature and a large exciton binding energy of 60 meV [1–3]. Various techniques have been employed to grow ZnO [3], such as hydrothermal method [4,5], magnetron sputtering [6,7], pulse laser deposition [8–10], metal-organic chemical vapor deposition [11–14], and molecular-beam epitaxy (MBE) [15–37]. Among these growth methods, MBE has some potential advantages, such as precise control of growth parameters and *in situ* characterization techniques. Although some other oxidants such as $NO_2$ [35], $O_3$ [36], and $H_2O_2$ [37] were tried, $O_2$ plasma-assisted method is the mainstream for ZnO MBE growth. Radio frequency (RF) and electron cyclotron resonance (ECR) are the two main plasma generation approaches. Generally ECR plasma [28–34] can sustain much larger $O_2$ flowing rate than RF plasma [20–27] during ZnO growth. So oxygen rich condition is easier to be achieved by ECR plasma-assisted MBE, which is very critical for *p*-type ZnO because of the suppression of zinc interstitials and oxygen vacancies [31,32]. Besides the general MBE growth parameters such as Zn cell temperature, $O_2$ flowing rate, and substrate temperature, ECR plasma power is also critical for MBE ZnO growth. However, no experimental studies have been reported. In this paper, the effect of ECR plasma power on the growth rate, structural, electrical, and optical properties of the ZnO thin films is reported.

## 2. Experiment

ZnO thin films were grown on *r*-plane sapphire substrates using ECR plasma-assisted MBE. A radical effusion cell filled with elemental Zn (6N) metals was used as Zn source. Zn flux is controlled by the effusion cell temperature. An ECR plasma tube supplied with $O_2$ (5N) gas was used as the oxygen source. Oxygen flow rate can be precisely tuned by a mass flow controller. The

* Corresponding author. Tel.: +1 951 8277131; fax: +1 951 8272425.
*E-mail address:* jianlin@ee.ucr.edu (J.L. Liu).

0169-4332/$ – see front matter © 2008 Elsevier B.V. All rights reserved.
doi:10.1016/j.apsusc.2008.09.068

Author's personal copy



**Table 1**
Growth parameters and growth rates of the ZnO thin films.

| Sample | Zn cell temperature (°C) | $O_2$ flow rate (sccm) | ECR current (mA) | ECR power (W) | Growth rate (nm/min) |
|---|---|---|---|---|---|
| A | 360 | 15 | 20 | 76 | 0.38 |
| B | 380 | 15 | 20 | 76 | 0.94 |
| C | 390 | 15 | 20 | 76 | 1.11 |
| D | 400 | 15 | 20 | 76 | 1.11 |
| E | 400 | 15 | 40 | 152 | 1.78 |
| F | 400 | 15 | 60 | 228 | 2.07 |
| G | 380 | 20 | 20 | 76 | 0.87 |

color of the oxygen plasma looks yellowish-white and white at small (e.g. 76 W) and large (e.g. 228 W) ECR powers, respectively. The sapphire substrates were cleaned by the following procedures before growth. Firstly, the substrate was chemically cleaned in the hot (~150 °C) aqua regia ($HNO_3$:HCl = 1:3) solutions for 20 min; rinsed by de-ionized water; dried by nitrogen gun; and transferred into the MBE chamber. Subsequently, the substrate was thermally cleaned by annealing it at 800 °C under vacuum in MBE chamber for 10 min. Finally, 10 min oxygen plasma exposure treatment was performed and the ZnO growth was immediately followed. The substrate temperature was kept at ~550 °C. Different growth conditions were employed by tuning the Zn cell temperature, $O_2$ flow rate, and ECR plasma power.

*In situ* reflection high-energy electron diffraction (RHEED) measurements were performed on the as grown samples. X-ray diffraction (XRD) measurements were performed using a Bruker D8 Advance X-ray diffractometer. Hall effect measurements were carried out using an Ecopia HMS-3000 Hall effect measurement system at room temperature. Photoluminescence (PL) study was carried out using a home-built PL system at room temperature. A 325-nm-wavelength He–Cd laser was used as excitation source and a photomultiplier tube was used to detect the PL signals.

## 3. Results and discussions

### 3.1. Growth rates

Table 1 shows the growth parameters and growth rates of the ZnO thin films. Samples A–D were grown with the same $O_2$ flow rate of 15 sccm and ECR plasma power of 76 W, but with different Zn effusion cell temperatures ranging from 360 to 400 °C. Samples D–F were grown with the same Zn effusion cell temperature at 400 °C and $O_2$ flow rate of 15 sccm, but with different ECR plasma powers, ranging from 76 to 228 W. Sample G was grown for comparison to sample B, which only differs in the oxygen flowing rate.

Fig. 1(a) shows the relation between the ZnO thin film growth rate and the Zn effusion cell temperature within samples A–D. The growth rate increases from 0.38 nm/min in sample A to 1.11 nm/min in sample C with the increase of the Zn cell temperature from 360 to 390 °C. However, further increase of the Zn cell temperature from 390 to 400 °C leads to the saturation of the growth rate, which means zinc rich condition has been reached. It is concluded that sample C was grown approximately under stoichiometric condition and oxygen rich condition is reached within the regime of Zn cell temperature between 360 and 390 °C. In the oxygen rich condition region, further increase of $O_2$ flow rate while maintaining the same Zn cell temperature (for example, 15 sccm for sample B vs. 20 sccm for sample G) leads to slightly smaller growth rate (0.87 nm/min for sample G and 0.94 nm/min for sample B). This is attributed to the larger scattering rate from increased gas flow. Fig. 1(b) shows the relation between the growth rate and the ECR plasma power within samples D–F. The growth rate increases from 1.11 nm/min in sample D to 2.07 nm/min in sample F with the increase of the ECR power from 76 to 228 W, indicating that ECR power plays an important role for ZnO thin film growth rate. The increase of the growth rate at the increased plasma power is attributed to the increased atomic oxygen density, because the Zn atoms react with the atomic oxygen instead of molecular oxygen during the ZnO growth. Similar experimental results were also reported in the ECR plasma-assisted MBE nitride growth that larger plasma power leads to increased density of the atomic nitrogen [38].

### 3.2. Structural properties

Fig. 2 shows the RHEED patterns of samples A–F. From A–C, the RHEED patterns become more and more streaky, indicating that

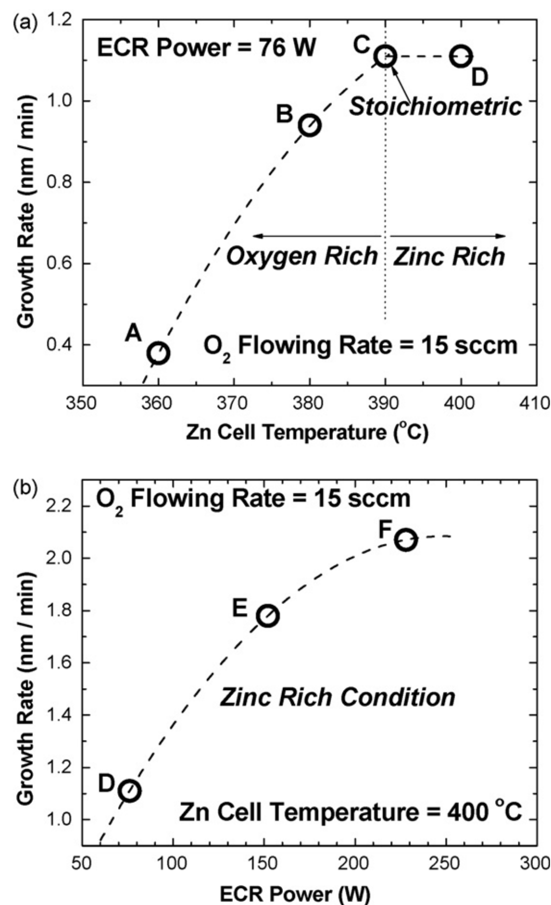


**Fig. 1.** (a) Growth rate as a function of Zn cell temperature. $O_2$ flow rate and ECR power were kept at constants of 15 sccm and 76 W, respectively. (b) Growth rate as a function of the ECR plasma power. $O_2$ flowing rate and Zn cell temperature were kept at constants of 15 sccm and 400 °C, respectively.

Author's personal copy



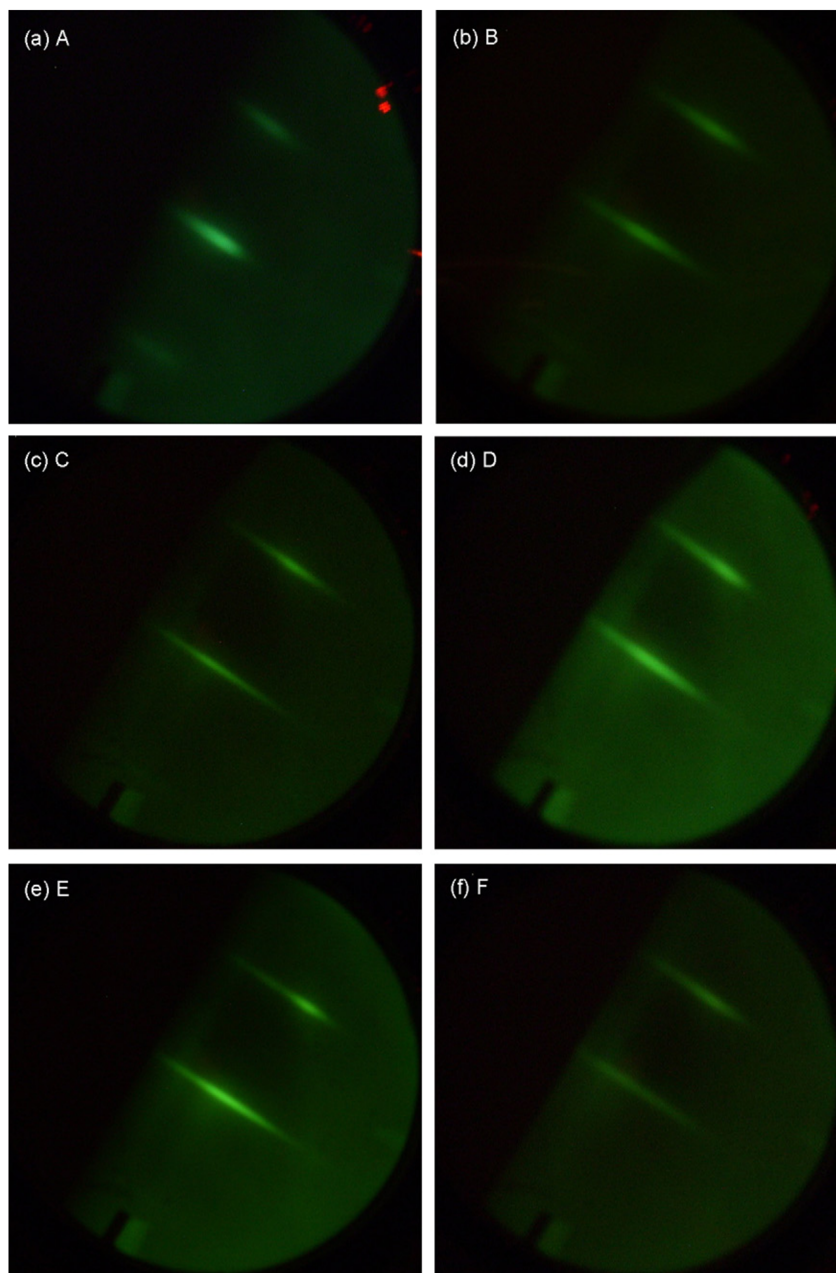


**Fig. 2.** (a)–(f) RHEED patterns of samples A–F, respectively. Samples A–D were grown with the same $O_2$ flow rate and ECR power but different Zn cell temperature. Samples A and B are under oxygen rich condition while sample D is under zinc rich condition. Sample C was grown with stoichiometric condition, showing the streakiest pattern. Samples D–F were grown with the same Zn cell temperature and oxygen flow rate but different ECR power. Samples D–F show similar RHEED pattern, indicating no evident roughness variation of the films with increased plasma power.

the surface is smoother. Also, sample C shows a streakier pattern than sample D. No evident RHEED pattern difference was observed among samples D–F, but differences were observed in the XRD spectra. Fig. 3 shows the XRD spectra of samples D–F. The peaks at 25.8° and 52.8° originate from the $(1\,\bar{1}\,0\,2)$ and $(2\,\bar{2}\,0\,4)$ planes of *r*-cut sapphire substrates. The peaks located at around 56.7° are from ZnO $(1\,1\,\bar{2}\,0)$ plane. The insets show the full width at half maximum (FWHM) of the $(1\,1\,\bar{2}\,0)$ ZnO peak, which decreases from 0.31° in sample D to 0.21° in sample F, indicating that larger ECR plasma power leads to better ZnO crystallinity. This is attributed to the decreased ionic oxygen (increased atomic oxygen) density from enhanced plasma power [38,39]. Ionic particles generally degrade thin film quality during the epitaxial growth. The FWHM values are also summarized in Table 3.

### 3.3. Electrical properties

Fig. 4(a) and (b) shows the relations between the electron carrier concentration and resistivity and the Zn cell temperature, respectively. The plasma power was fixed for all samples. Larger electron carrier concentration and lower resistivity were observed in thin film samples grown with higher Zn cell temperature, which was attributed to the larger density of Zn interstitials. Fig. 5(a) and (b) shows the relations between the electron carrier concentration and resistivity and the ECR oxygen plasma power, respectively, with the Zn cell temperature at constant. Smaller electron carrier concentration and higher resistivity were observed in thin film samples grown with larger plasma power, which was attributed to the

Author's personal copy



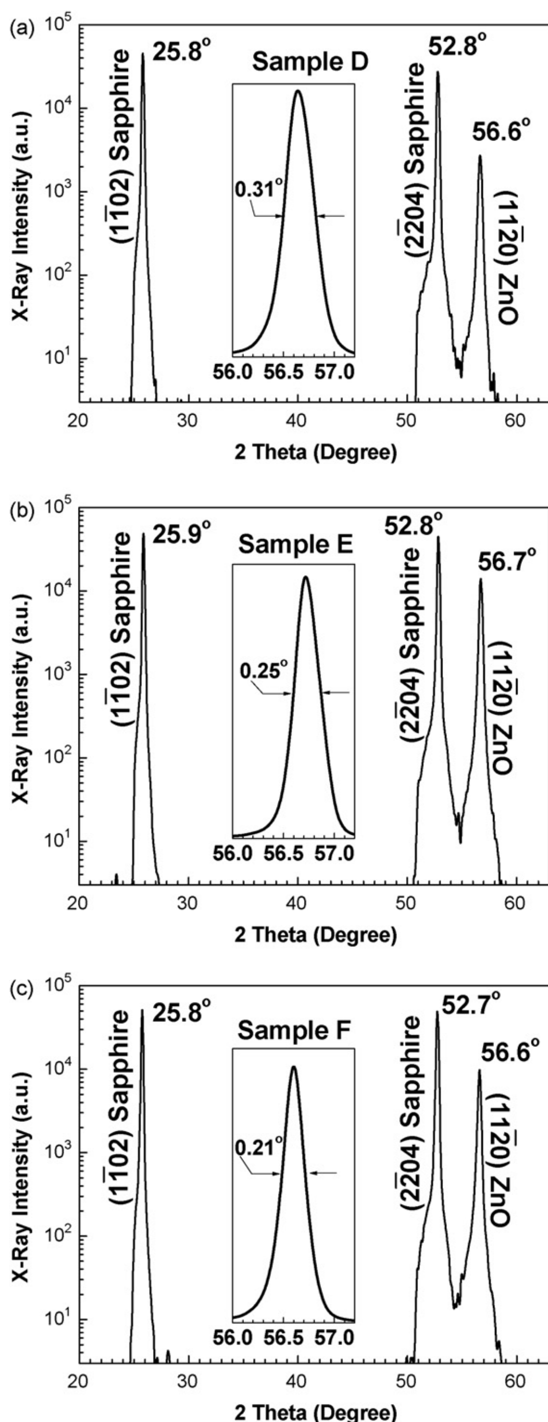

**Fig. 3.** XRD spectra of samples D–F. The insets show FWHM of the $(1\,1\,\bar{2}\,0)$ ZnO peak, which decreases from 0.31° to 0.21° from sample D to F, indicating better crystallinity.

suppression of Zn interstitial formation with increased plasma power. When the ECR oxygen plasma power increases, although the oxygen flow rate does not increase, the atomic oxygen supply increases. This suggests that during plasma-assisted MBE ZnO growth, oxygen rich condition can be obtained not only by decreasing Zn cell temperature or increasing oxygen flow rate, but also by increasing oxygen plasma power. Hall effect measurements results of the ZnO thin films were also summarized in Table 2.

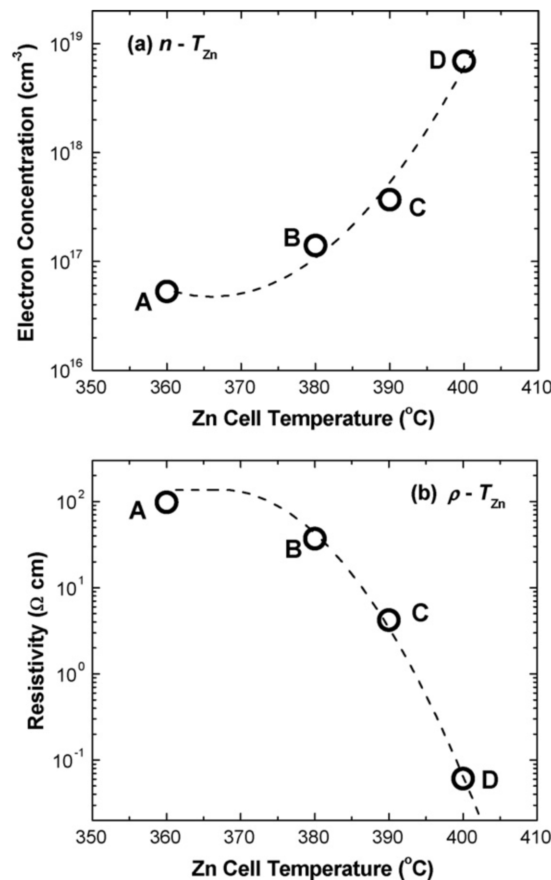

**Fig. 4.** (a) Electron carrier concentration as a function of Zn cell temperature with plasma power at constant. (b) Resistivity as a function of Zn cell temperature with plasma power at constant. Larger electron carrier concentration and lower resistivity were observed in thin film samples grown with higher Zn cell temperature, which was attributed to the larger density of Zn interstitials.

### 3.4. Optical properties

Fig. 6 shows room-temperature PL spectra of samples D–F. The peaks around 3.30 eV are from ZnO near band-edge (NBE) emission. FWHM of the ZnO NBE emission peaks decreases from 190 to 175 meV from samples D to F. FWHM values of the PL peaks were also summarized in Table 3. Narrow room temperature PL peak width indicates small density of non-radiative centers. So it shows that better optical properties can be achieved with larger ECR oxygen plasma power during ZnO growth. The reason is also attributed to the decreased ionic oxygen density from enhanced plasma power. The decreased ionic oxygen reduces the crystalline degradation of the ZnO film arising from the ionic oxygen hitting the film surface during growth. The density of the non-radiative centers of epitaxial grown materials is closely related to the crystallinity.

## 4. Summary

ZnO thin films were grown on sapphire substrates using ECR plasma-assisted MBE. ECR plasma power plays an important role to the growth rate and crystallinity of ZnO thin films. The growth rate increases with the increase of plasma power because of the increased atomic oxygen density. The enhanced plasma power improves ZnO film crystallinity, decreases the density of Zn interstitial defect formation, and improves optical properties because of decreased ionic oxygen density.

Author's personal copy



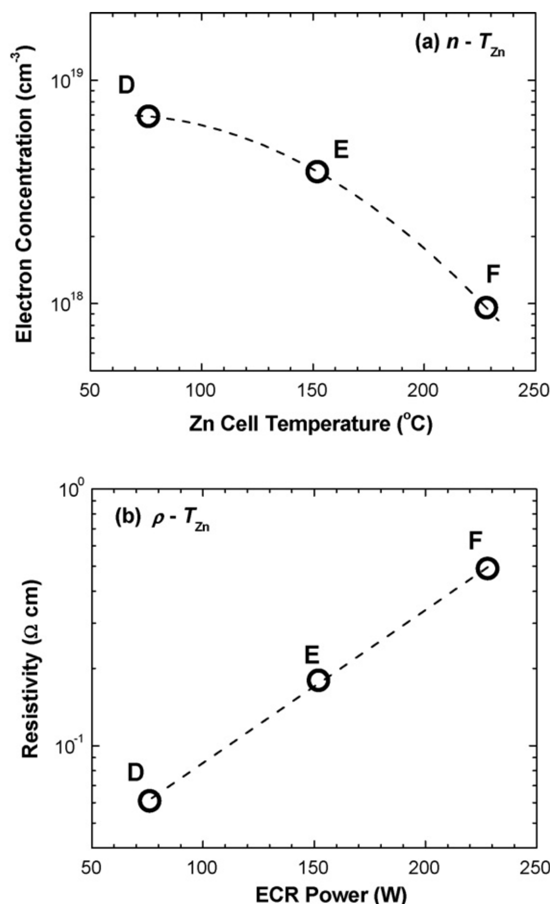


**Fig. 5.** (a) Electron carrier concentration as a function of plasma power with Zn cell temperature at constant. (b) Resistivity as a function of plasma power with Zn cell temperature at constant. Smaller electron carrier concentration and higher resistivity were observed in thin film samples grown with larger plasma power, which was attributed to the suppression of Zn interstitial formation with increased plasma power.

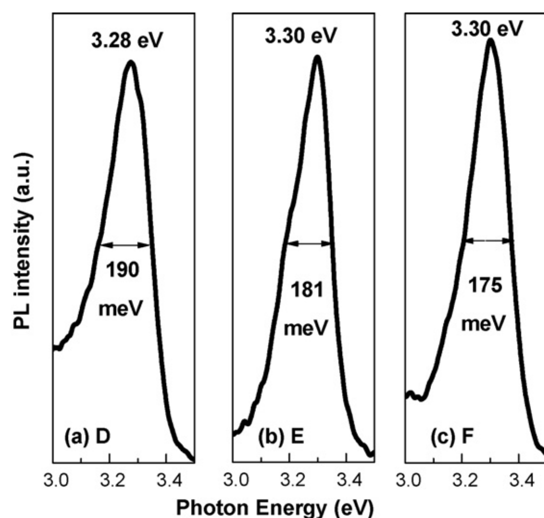


**Fig. 6.** Room-temperature PL emission spectra of samples D–F around the NBE region. The FWHM of the ZnO NBE emission peaks decreases from 190 to 175 meV with increased plasma power from samples D to F.

**Table 2**
Hall effect measurements data of the ZnO thin films.

| Sample | Electron carrier concentration ($cm^{-3}$) | Resistivity ($\Omega$ cm) | Hall mobility ($cm^2$/V s) |
|---|---|---|---|
| A | $5.3 \times 10^{16}$ | 98 | 1.2 |
| B | $1.4 \times 10^{17}$ | 37 | 1.2 |
| C | $3.7 \times 10^{17}$ | 4.2 | 4.0 |
| D | $6.9 \times 10^{18}$ | 0.061 | 15 |
| E | $3.9 \times 10^{18}$ | 0.18 | 8.8 |
| F | $9.6 \times 10^{17}$ | 0.49 | 13 |

**Table 3**
Full-width at half-maximum (FWHM) of the ZnO $(1 1 \bar{2} 0)$ XRD and near band emission (NBE) PL peaks from the ZnO thin film samples D–F at room temperature.

| Sample | FWHM of ZnO $(1 1 \bar{2} 0)$ XRD peak (°) | FWHM of ZnO NBE PL peak (meV) |
|---|---|---|
| D | 0.31 | 190 |
| E | 0.25 | 181 |
| F | 0.21 | 175 |


## Acknowledgement

This work was supported by ONR/DMEA through the Center of Nanomaterials and Nanodevice (CNN) under the award no. H94003-08-2-0803.


## References


[1] D.C. Look, Mater. Sci. Eng. B 80 (2001) 383.
[2] S.J. Pearton, D.P. Norton, K. Ip, Y.W. Heo, T. Steiner, J. Vac. Sci. Technol. B 22 (2004) 932.
[3] Ü. Özgür, Ya.I. Alivov, C. Liu, A. Teke, M.A. Reshchikov, S. Doğan, V. Avrutin, S.-J. Cho, H. Morkoç, J. Appl. Phys. 98 (2005) 041301.
[4] T. Sekiguchi, S. Miyashita, K. Obara, T. Shishido, N. Sakagami, J. Crystal Growth 214/215 (2000) 72.
[5] E. Ohshima, H. Ogino, I. Niikura, K. Maeda, M. Sato, M. Ito, T. Fukuda, J. Crystal Growth 264 (2004) 166.
[6] Z.C. Jin, I. Hamberg, C.G. Granqvist, J. Appl. Phys. 64 (1988) 5117.
[7] K.B. Sundaram, A. Khan, Thin Solid Films 295 (1997) 87.
[8] X.W. Sun, H.S. Kwok, J. Appl. Phys. 86 (1999) 408.
[9] B.J. Jin, S.H. Bae, S.Y. Lee, S. Im, Mater. Sci. Technol. B 71 (2000) 301.
[10] B.J. Jin, S. Im, S.Y. Lee, Thin Solid Films 366 (2000) 107.
[11] C.R. Gorla, N.W. Emanetoglu, S. Liang, W.E. Mayo, Y. Lu, M. Wraback, H. Shen, J. Appl. Phys. 85 (1999) 2595.
[12] Y. Liu, C.R. Gorla, S. Liang, N. Emanetoglu, Y. Lu, H. Shen, M. Wraback, J. Electron. Mater. 29 (2000) 69.
[13] J. Ye, S. Gu, S. Zhu, T. Chen, L. Hu, F. Qin, R. Zhang, Y. Shi, Y. Zheng, J. Crystal Growth 243 (2002) 151.
[14] Z. Fu, B. Lin, J. Zu, Thin Solid Films 402 (2002) 302.
[15] M.A.L. Johnson, S. Fujita, W.H. Rowland Jr., W.C. Hughes Jr., J.W. Cook, J.F. Schetzina, J. Electron. Mater. 25 (1996) 855.
[16] D.M. Bagnall, Y.F. Chen, Z. Zhu, T. Yao, S. Koyama, M.Y. Shen, T. Goto, Appl. Phys. Lett. 70 (1997) 2230.
[17] P. Zu, Z.K. Tang, G.K.L. Wong, M. Kawasaki, A. Ohtomo, H. Koinuma, Y. Segawa, Solid State Commun. 103 (1997) 459.
[18] Z.K. Tang, G.K.L. Wong, P. Yu, M. Kawasaki, A. Ohtomo, H. Koinuma, Y. Segawa, Appl. Phys. Lett. (1998) 3270.
[19] Y. Chen, D.M. Bagnall, H. Koh, K. Park, K. Hiraga, Z. Zhu, T. Yao, J. Appl. Phys. 84 (1998) 3912.
[20] H. Kato, M. Sano, K. Miyamoto, T. Yao, Jpn. J. Appl. Phys. 42 (2003) 2241.
[21] F. Vigué, P. Vennéguès, S. Vézian, M. Laügt, J.-P. Faurie, Appl. Phys. Lett. 79 (2001) 194.
[22] T. Ohgaki, N. Ohashi, H. Kakemoto, S. Wada, Y. Adachi, H. Haneda, T. Tsurumi, J. Appl. Phys. 93 (2003) 1961.
[23] K. Nakahara, T. Tanabe, H. Takasu, P. Fons, K. Iwata, A. Yamada, K. Matsubara, R. Hunger, S. Niki, Jpn. J. App. Phys. 40 (2001) 250.
[24] F.X. Xiu, Z. Yang, L.J. Mandalapu, J.L. Liu, W.P. Beyermann, Appl. Phys. Lett. 88 (2006) 052106.
[25] F.X. Xiu, Z. Yang, L.J. Mandalapu, J.L. Liu, W.P. Beyermann, Appl. Phys. Lett. 88 (2006) 152116.
[26] Z. Yang, J.L. Liu, M. Biasini, W.P. Beyermann, Appl. Phys. Lett. 92 (2008) 042111.
[27] Z. Yang, J.L. Liu, D.C. Look, unpublished.
[28] T.E. Murphy, D.Y. Chen, E. Cagin, J.D. Phillips, J. Vac. Sci. Technol. B 23 (2005) 1277.
[29] K. Nakamura, T. Shoji, H.-B. Kang, Jpn. J. Appl. Phys. 39 (2000) L534.
[30] I. Sakaguchi, H. Ryoken, S. Hishita, H. Haneda, Thin Solid Films 506/507 (2006) 184.

Author's personal copy



[31] F.X. Xiu, Z. Yang, L.J. Mandalapu, D.T. Zhao, J.L. Liu, W.P. Beyermann, Appl. Phys. Lett. 87 (2005) 152101.
[32] F.X. Xiu, Z. Yang, L.J. Mandalapu, D.T. Zhao, J.L. Liu, Appl. Phys. Lett. 87 (2005) 252102.
[33] F. Xiu, Z. Yang, D. Zhao, J. Liu, K.A. Alim, A.A. Balandin, M.E. Itkis, R.C. Haddon, J. Crystal Growth 286 (2006) 61.
[34] F.X. Xiu, Z. Yang, D.T. Zhao, J.L. Liu, K.A. Alim, A.A. Balandin, M.E. Itkis, R.C. Haddon, J. Electron. Mater. 35 (2006) 691.
[35] K. Sakurai, D. Iwata, S. Fujita, S. Fujita, Jpn. J. Appl. Phys. 38 (1999) 2606.
[36] M. Fujita, N. Kawamoto, T. Tatsumi, K. Yamagishi, Y. Horikoshi, Jpn. J. Appl. Phys. 42 (2003) 67.
[37] N. Izyumskaya, V. Avrutin, W. Schoch, A. El-Shaer, F. Reuß, Th. Gruber, A. Waag, J. Crystal Growth 269 (2004) 356.
[38] M. Meyyappan, J. Nitride Semiconductor Res. 2 (1997) 46.
[39] R.J. Molnar, T.D. Moustakas, J. Appl. Phys. 76 (1994) 4587.